Evolution of Specialization in Heterogeneous Environments: Equilibrium Between Selection, Mutation and Migration

Sepideh Mirrahimi,* and Sylvain Gandon[†,1]

*Institut de Mathématiques de Toulouse, UMR5219, Université de Toulouse, CNRS, UPS, IMT, F-31062 Cedex 9, France and [†]CEFE, Université de Montpellier, CNRS, EPHE, IRD, University Paul Valéry, 34293 Montpellier 3, France

ORCID ID: 0000-0003-2624-7856 (S.G.)

ABSTRACT Adaptation in spatially heterogeneous environments results from the balance between local selection, mutation, and migration. We study the interplay among these different evolutionary forces and demography in a classical two-habitat scenario with asexual reproduction. We develop a new theoretical approach that goes beyond the Adaptive Dynamics framework, and allows us to explore the effect of high mutation rates on the stationary phenotypic distribution. We show that this approach improves the classical Gaussian approximation, and captures accurately the shape of this equilibrium phenotypic distribution in one- and two-population scenarios. We examine the evolutionary equilibrium under general conditions where demography and selection may be nonsymmetric between the two habitats. In particular, we show how migration may increase differentiation in a source–sink scenario. We discuss the implications of these analytic results for the adaptation of organisms with large mutation rates, such as RNA viruses.

KEYWORDS local adaptation; migration-selection balance; gene flow; Adaptive Dynamics; Quantitative Genetics; skew

SPATIALLY heterogeneous selection is ubiquitous, and constitutes a potent evolutionary force that promotes the emergence and the maintenance of biodiversity. Spatial variation in selection can yield adaptation to local environmental conditions; however, other evolutionary forces, like migration and mutation, tend to homogenize the spatial patterns of differentiation, and thus impede the build up of local adaptation. Understanding the balance between these contrasting evolutionary forces is a major objective of evolutionary biology theory (Slatkin 1978; Savolainen *et al.* 2013; Whitlock 2015) and could lead to a better understanding of the speciation process and the evolutionary response to global change (Doebeli and Dieckmann 2003; Leimar *et al.* 2008. In this article, we consider a two-habitat model with explicit demographic dynamics as in Meszéna *et al.* (1997), Day (2000), Ronce and Kirkpatrick (2001), and Débarre *et al.* (2013). We assume that adaptation is governed by a single quantitative trait where individuals reproduce asexually. Maladapted populations have a reduced growth rate, and, consequently, lower population size. In other words, selection is assumed to be "hard" (Christiansen 1975; Débarre and Gandon 2010) as the population size in each habitat is affected by selection, mutation, and migration. These effects are complex because, for instance, nonsymmetric population sizes affect gene flow and adaptation feeds back on demography and population sizes (Nagylaki 1978; Meszéna *et al.* 1997; Day 2000; Ronce and Kirkpatrick 2001; Lenormand 2002; Débarre *et al.* 2013). To capture the complexity of these feed backs, it is essential to keep track of both the local densities and the distributions of phenotypes in each habitat. Note that this complexity often led to the analysis of the simplest ecological scenarios, where the strength of selection, migration, and demographic constraints are assumed to be the same in the two habitats (we will refer to such situations as symmetric scenarios). See, however, Holt and Gaines (1992), García-Ramos and Kirkpatrick (1997), Gomulkiewicz *et al.* (1999), and Holt *et al.* (2003) for the analysis of the effect of asymmetric migration from a source habitat on the dynamics of adaptation in a peripheral (*i.e.*, sink) habitat. Three different approaches have been used to analyze these two-population

models. Each of these approaches rely on a set of restrictive assumptions regarding the relative influence of the different evolutionary forces acting on the evolution of the population.

First, under the assumption that the rate of mutation is weak relative to selection, it is possible to use the Adaptive Dynamics framework [see Meszéna *et al.* (1997); Day (2000); Szilágyi and Meszéna (2009); Débarre *et al.* (2013), but also *Results* for a presentation of this framework]. This analysis captures the effect of migration and selection on the long-term evolutionary equilibrium. In particular, this approach shows that weak migration relative to selection promotes the coexistence of two specialist strategies (locally adapted to each habitat). In contrast, when migration is strong relative to selection, a single generalist strategy is favored. The main limitation of this approach is that it relies on the assumption that the mutation rate is vanishingly small, which results in a very limited amount of genetic variability. At most, two genotypes can coexist in this two-habitat model.

Second, Quantitative Genetics formalism, based on computation of the moments of phenotypic distribution, has been used to track evolutionary dynamics in heterogeneous habitats when there is a substantial level of phenotypic diversity in each population (Ronce and Kirkpatrick 2001). This model considers sexual reproduction with a quantitative trait [considering multiple loci with small effects (Fisher 1919)]. However, similar types of equations, describing the dynamics of the moments of phenotypic distribution, can also be derived in the case of asexual reproduction considering large mutation rates [see Débarre *et al.* (2013) and below]. This formalism allows the recovery of classical migration thresholds below which specialization is feasible. But the analysis of Ronce and Kirkpatrick (2001) also reveals the existence of evolutionary bistability, where transient perturbations of the demography can have long-term evolutionary consequences for specialization. Yet, the assumption of the shape of the phenotypic distribution (assumed to be Gaussian in each habitat) is a major limitation of this formalism.

Third, attempts to account for other shapes of phenotypic distributions in heterogeneous environments have been developed recently (Yeaman and Guillaume 2009; Débarre *et al.* 2013, 2015). These models highlight that calculations based on the Gaussian approximation, which neglects the skewness of the equilibrium phenotypic distribution, underestimate the level of phenotypic divergence and local adaptation. Yet, there is currently no model able to accurately describe the build up of non-Gaussian distributions. The only attempts to model this distribution describe the phenotypic distributions in each habitat as the sum of two Gaussian distributions Yeaman and Guillaume 2009; Débarre *et al.* 2013. These models, however, yield only approximate predictions on long-term evolutionary equilibria.

Here, we develop an alternative formalism that yields population size and phenotypic distribution in each habitat at the equilibrium between selection, mutation, and migration. In *Materials and Methods*, we present our two-population model. For heuristic reasons, we next provide analysis of the equilibrium between selection and mutation in a single population. This provides an illustration of our approach in a simple scenario, and shows how this analysis can go beyond the classical Gaussian approximation. Next, we extend this approach to a two-population scenario, where migration can also influence phenotypic distribution, and we derive approximations for the level of adaptation under a migration–selection–mutation balance. We also explore the effects of nonsymmetric constraints on selection, migration, or demography between the two habitats. We evaluate the accuracy of these approximations by comparing them to numerical solutions of our deterministic model, and we show that our approach improves previous attempts to study the interplay between adaptation and demography in heterogeneous environments. We contend that our results are particularly relevant for organisms with high mutation rates and may help to understand the within-host dynamics of chronic infections by RNA viruses (Drake and Holland 1999; Sanjuán *et al.* 2010).

The present work has been prepared in parallel to the mathematical article Mirrahimi 2017 where we provide the mathematical basis and proofs for the method used here. See also Gandon and Mirrahimi (2017), where those mathematical results were announced. The aim of the present paper is to show how this approach can help to understand the balance between different evolutionary forces. We present several new biological scenarios, and derive new results that help grasp the interplay between different evolutionary forces and demography.

Materials and Methods

We model an environment containing two habitats that we label 1 and 2 (Figure 1). The population is structured by a quantitative trait z. In each habitat i there is stabilizing selection on the trait z for an optimal value θ_i (for habitat $i = 1, 2$). The growth rate in habitat i is denoted by $r_i(z)$, which has its maximum $r_{\max,i}$ when $z = \theta_i$. In the following, we will focus mainly on the following quadratic stabilizing selection function (Bürger 2000, pp. 117–121 and chapter VI):

$$r_i(z) = r_{\max,i} - s_i(z-\theta_i)^2. \tag{1}$$

We denote by s_i the selection pressure in habitat i. Without loss of generality, we assume that $\theta_1 = -\theta_2 = -\theta$. But our approach could be used with other stabilizing selection functions (see Equation 12 below, where another selection function is studied in the case of one population).

Reproduction is assumed to be asexual. Offspring inherit the phenotype of their parent (*i.e.*, no environmental variance), and we consider a continuum of alleles model (Kimura 1965). Mutations occur with a constant rate U (*i.e.*, mutations are not associated with reproduction), and add an increment y to the parents' phenotype; we assume that the distribution of these mutational effects is given by $K(y)$, with mean 0 and variance equal to $2V_m$. We also

assume that individuals disperse out of habitat i with rate m_i. Rates of migration are assumed to be independent of individuals' phenotypes.

Let $n_i(t, z)$ be the phenotypic density in habitat i at time t. The dynamics of this density in each habitat is given by (for $i = 1, 2$ and $j = 2, 1$):

$$\frac{\partial n_i(t,z)}{\partial t} = \underbrace{U\left(\int_{-\infty}^{+\infty} n_i(t, z-y)K(y)dy - n_i(t,z)\right)}_{\text{mutation}}$$
$$+ \underbrace{n_i(t,z)\left(r_i(z) - \kappa_i \int_{-\infty}^{+\infty} n_i(t,y)dy\right)}_{\text{growth}} \quad (2)$$
$$+ \underbrace{m_j n_j(t,z) - m_i n_i(t,z)}_{\text{migration}}.$$

The first term on the right-hand side of the above equation corresponds to the effect of mutations. The second term corresponds to the logistic growth that results from the balance between reproduction given by Equation 1 and density dependence, where κ_i measures the intensity of competition within each habitat. The last term corresponds to the dispersal of individuals between habitats.

If we assume that the variance of the mutation distribution is small relative to the mutation rate U, we can consider an approximate model where we replace the mutation term in Equation 2 by a diffusion [see Kimura (1965); Lande (1975) and the more recent article by Champagnat *et al.* 2008, where the diffusion term has been derived directly from a stochastic individual based model]. See also Bürger (2000, pp. 239–241) for a discussion on the domain of the validity of such model. Our model then becomes:

$$\frac{\partial n_i(t,z)}{\partial t} = UV_m \frac{\partial^2 n_i(t,z)}{\partial z^2} + n_i(t,z)\left(r_i(z) - \kappa_i \int_{-\infty}^{+\infty} n_i(t,y)dy\right)$$
$$+ m_j n_j(t,z) - m_i n_i(t,z).$$
$$(3)$$

The total population sizes in each habitat is given by:

$$N_i(t) = \int_{-\infty}^{+\infty} n_i(t,z)dz, \qquad \text{for } i = 1, 2. \quad (4)$$

In other words, $n_i(t, z)$ refers to the density of individuals with phenotype z in habitat i, while N_i refers to the total density of the polymorphic population in habitat i.

Data availability statement

Results

One population: the selection–mutation equilibrium

In this section, we start by a simple scenario with no migration. This one-population example provides a good introduction to our method. The dynamics of the phenotypic density in a single habitat is given by:

$$\frac{\partial n_0(t,z)}{\partial t} = UV_m \frac{\partial^2 n_0(t,z)}{\partial z^2} + n_0(t,z)(r_0(z) - \kappa N_0(t)), \quad (5)$$

where N_0 is the total population size:

$$N_0(t) = \int_{-\infty}^{+\infty} n_0(t,y)dy.$$

For this scenario, we consider a more general form of growth rate $r_0(z)$ than in Equation 1. We suppose only that $r_0(z)$ is maximized for an optimal trait z_0. In the following, we present our two-step approach. First, we analyze the evolutionary equilibria of the problem when the rate of mutation is small, and we identify the evolutionary stable strategy (ESS). Second, we use this ESS to derive an approximation for the stationary solution of Equation 5 when mutation is more frequent and maintains a standing variance at equilibrium.

Adaptive dynamics and ESSs

In this section, we assume that mutations are very rare, such that a mutation is fixed or goes extinct before a new mutation arises in the population. The phenotypic distribution results from a collection of spikes. Such spikes are gradually replaced by others with the arrival of new mutations and through a competitive procedure. The theory of Adaptive Dynamics (Geritz *et al.* 1998) is based on the study of the stable equilibrium distribution and the localization of the spikes of such equilibrium, known as ESSs. Note that, in this first step, we do not make any assumption regarding the effects of these mutations on the phenotype. We are interested in the identification of the global ESSs, *i.e.*, when the resident population cannot be invaded by any mutation, no matter what its effect.

In absence of migration, the phenotype z_0 constitutes a globally stable evolutionary strategy. Indeed, when such monomorphic population reaches its demographic equilibrium, the total population size is given by $N_0^* = \frac{r(z_0)}{\kappa}$. The fate of a mutant with phenotype z_m introduced into such a resident population is determined by its fitness (*i.e.*, per capita growth rate minus density dependence) given by:

$$w\left(z_m; N_0^*\right) = r_0(z_m) - \kappa_0 N_0^* < w\left(z_0; N_0^*\right) = 0. \quad (6)$$

No mutant trait z_m can indeed invade the population since $r_0(z)$ takes its maximum at z_0.
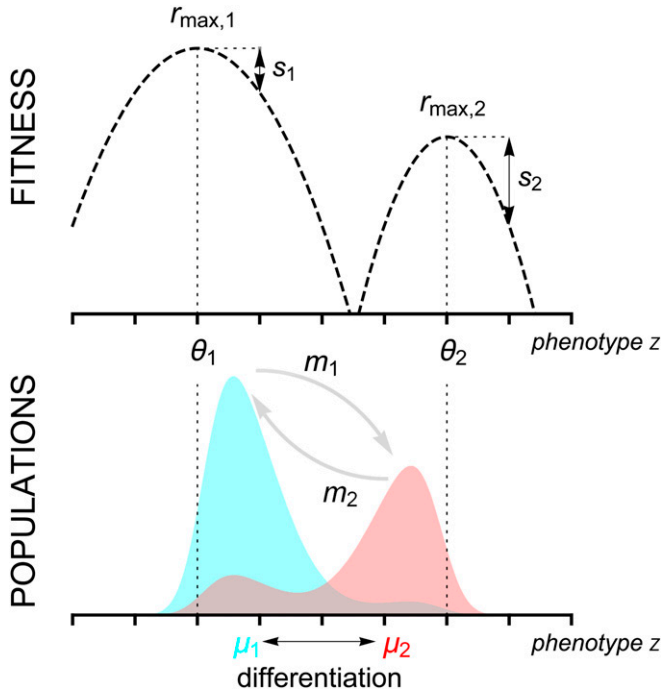
Figure 1 Schematic representation of the two habitat model. The top figure shows the growth rate (fitness) in each habitat as a function of the phenotypic trait z. In habitat i, the growth rate is assumed to be maximized at $z = \theta_i$, and the strength of selection is governed by s_i (see Equation 1). Here, we illustrate a scenario with nonsymmetric fitness functions. The bottom figure shows the phenotypic density in each habitat (light blue and light red in habitats 1 and 2, respectively). Migration from population i is governed by the parameter m_i, and tends to reduce the differentiation (*i.e.*, the difference between the mean phenotypes) between populations.

Equilibrium distribution with mutation

The ESS z_0 corresponds to the long-term evolutionary outcome in a scenario where all phenotypic strategies are present initially, but where mutation is absent. In the following, we study the impact of mutation on the ultimate evolutionary equilibrium of the population.

We introduce a new parameter, $\varepsilon = \sqrt{V_m}$. Hence, we replace V_m by ε^2, and we approximate the phenotypic density $n_{\varepsilon,0}^*(z)$, the equilibrium of Equation 5, in terms of ε (where the subscript ε in $n_{\varepsilon,0}^*$ indicates the dependence of the phenotypic density on the parameter ε). Our objective is to provide an approximation of the phenotypic density when the effect of mutation (measured by ε) is small, while the mutation rate can be large.

To study $n_{\varepsilon,0}^*(z)$, we will use a method based on Hamilton-Jacobi equations (see Equation A.5), which was developed by the mathematical community during the last decade to study selection–mutation models, when the effect of mutations is vanishingly small. This method was first suggested by Diekmann *et al.* (2005), and was developed for the case of homogeneous environments in Perthame and Barles (2008) and Barles *et al.* (2009). However, those works, which are addressed to the mathematical community, were focused mainly on the limited case where the effect of mutations, ε,

is vanishingly small. Here, we go further than previous studies, and characterize the phenotypic distribution when the mutations have non-negligible effects.

The method is based on the following transformation:

$$n_{\varepsilon,0}^*(z) = \frac{1}{\sqrt{2\pi\varepsilon}} \exp\left(\frac{u_{\varepsilon,0}(z)}{\varepsilon}\right). \tag{7}$$

The introduction of the function $u_{\varepsilon,0}(z)$ is a mathematical trick. It is indeed easier to first provide an approximation of $u_{\varepsilon,0}(z)$ rather than directly studying $n_{\varepsilon,0}^*(z)$.

Note that a first approximation of the population's phenotypic density, which is commonly used in the theory of Quantitative Genetics, is a Gaussian approximation of the following form around z^*:

$$n_{\varepsilon,0}^*(z) \approx N_{\varepsilon,0}^* \, \mathcal{N}\left(z^*, \varepsilon \, \sigma^2\right). \tag{8}$$

The Gaussian approximation is as if we had imposed $u_{\varepsilon,0}(z)$ to be a quadratic function of z, that is $u_{\varepsilon,0}(z) = \varepsilon \log\left(\frac{N_{\varepsilon,0}^*}{\sigma}\right) - \frac{(z-z^*)^2}{2\sigma^2}$. Our objective, however, is to obtain more accurate results than Equation 8, and to approximate $u_{\varepsilon,0}$ without making an *a priori* Gaussian assumption. To this end, we postulate an expansion for $u_{\varepsilon,0}(z)$ in terms of ε:

$$u_{\varepsilon,0}(z) = u_0(z) + \varepsilon v_0(z) + O\left(\varepsilon^2\right), \tag{9}$$

and we try to compute the coefficients $u_0(z)$ and $v_0(z)$. These terms can indeed be computed explicitly, and they lead to an approximation of the total population size N_ε^* and the phenotypic density $n_\varepsilon^*(z)$, which we will henceforth call our *first approximation* (see the supplementary information A.1.1 for these derivations).

In order to provide more explicit formula for the moments of order $k \geq 1$ of the population's distribution in terms of the parameters of the model, we also provide a *second approximation*. This *second approximation*, instead of using the values of u_0 and v_0 in the whole domain, is based on the Taylor expansions of u_0 and v_0 around the ESS points (see the supplementary information, Section A.1.2). Our *second approximation* is, by definition, less accurate than the first. We illustrate below the quality of these different approximations under two different scenarios.

Quadratic growth rate: We first consider a quadratic growth rate as in Equation 1:

$$r_0(z) = r_{\max,0} - s_0(z - \theta_0)^2. \tag{10}$$

In this case, our *first approximation* yields the Gaussian distribution (Equation 8) with:

$$N_{\varepsilon,0}^* \approx \frac{1}{\kappa_0}\left(r_{\max,0} - \varepsilon\sqrt{s_0 U}\right), \qquad \sigma^2 \approx \frac{\sqrt{U}}{\sqrt{s_0}}. \tag{11}$$

Note that this Gaussian distribution is actually an exact equilibrium of Equation 3, and the above $\approx$ signs can indeed

be replaced by equalities [see Kimura (1965) and Bürger (2000, Chapter IV)]. For the derivation of this result, see the supplementary information, Section A.1.1.

An asymmetric growth rate: We next consider a growth rate that is not symmetric:

$$r_0(z) = r_{\max,0} - s_0(z-\theta_0)^2\Big(a + (z-\theta_0-b)^2\Big). \quad (12)$$

In this case, the phenotypic distribution does not have a Gaussian profile, and our approximation yields:

$$N^*_{\varepsilon,0} \approx \frac{1}{\kappa_0}\Big(r_{\max,0} - \sqrt{s_0 U\Big(a+b^2\Big)}\ \varepsilon\Big),$$

$$n^*_{\varepsilon,0}(z) \approx \frac{1}{\sqrt{2\pi\varepsilon}}\exp\Big(\frac{u_0(z) + \varepsilon v_0(z)}{\varepsilon}\Big),$$

where the values of u_0 and v_0 can be computed explicitly (see the supplementary information, Section A.1.1). In Figure 2 we plot this *first approximation*, and compare it with the exact distribution that we derived numerically.

We can also use our *second approximation* to obtain analytic expressions for the mean phenotypic trait (see the supplementary information, Section A.1.2 for the derivation):

$$\mu^*_{\varepsilon,0} = \frac{1}{N^*_{\varepsilon,0}}\int z n^*_{\varepsilon,0}(z)dz = \theta_0 + \frac{2b\sqrt{U}\varepsilon}{\sqrt{s_0}\big(a+b^2\big)^{3/2}} + O\big(\varepsilon^2\big),$$

the mean variance:

$$\sigma^{*2}_{\varepsilon,0} = \frac{1}{N^*_{\varepsilon,0}}\int\Big(z-\mu^*_{\varepsilon,0}\Big)^2 n^*_{\varepsilon,0}(z)dz = \frac{\sqrt{U}\varepsilon}{\sqrt{s_0\big(a+b^2\big)}} + O\big(\varepsilon^2\big),$$

and the third central moment:

$$\psi^*_{\varepsilon,0} = \frac{1}{N^*_{\varepsilon,0}}\int\Big(z-\mu^*_{\varepsilon,0}\Big)^3 n^*_{\varepsilon,0}(z)dz = \frac{2bU\varepsilon^2}{s_0\big(a+b^2\big)^2} + O\big(\varepsilon^3\big).$$

In Table 1, we show that our two approximations capture accurately the first three moments of the equilibrium distribution using the parameters that we used in Figure 2. As expected, the *first approximation* is more accurate, but the analytic expressions of the *second approximation* given above allow us to capture the influence of the parameters of the model.

Two populations: the selection–mutation–migration equilibrium

Next, we return to analysis of the stationary solution of Equation 3, which results from the equilibrium between selection, mutation, and migration in each habitat. Using Equation 1 and Equation 3, one can derive dynamical equations for the size of the population and the mean phenotype ($\mu_i = \frac{1}{N_i}\int z n_i(t,z)dz$):
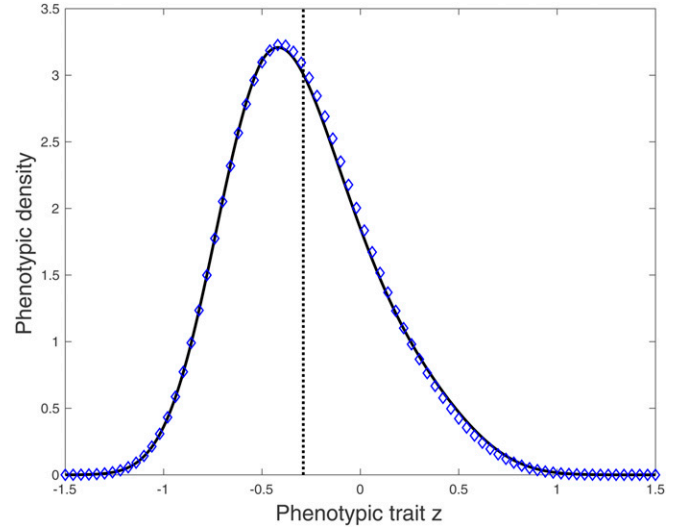

Figure 2 The selection–mutation equilibrium of the phenotypic density $n_{\varepsilon,0}(z)$ in a single population. We plot the exact phenotypic density at equilibrium obtained from numerical computations of the equilibrium of Equation 5 (blue dots) together with our *first approximation* (full black line) with the growth rate given in Equation 12. The vertical dotted line indicates the mean of the phenotypic distribution. Note the skewness of the equilibrium distribution that is accurately captured with our approximation (see also Table 1). In this figure, to compute the equilibrium numerically, we solved the dynamic problem numerically (Equation 5) and kept the solution obtained for a long time after the equilibrium has been reached. Parameter values: $r_{\max} = 3$, $s_0 = 1$; $\theta = -0.5$, $\kappa = 1$, $a = 0.2$, $b = 1$, $U = 1$, $\varepsilon = 0.1$.

$$\frac{d}{dt}N_i = N_i\big(r_{\max,i} - \kappa_i N_i\big) - s_i N_i\Big((\mu_i-\theta_i)^2+\sigma_i^2\Big)$$
$$\qquad + m_j N_j - m_i N_i,$$
$$\frac{d}{dt}\mu_i = -s_i\big(2(\mu_i-\theta_i)\sigma_i^2 + \psi_i\big) + m_j\frac{N_j}{N_i}\big(\mu_j - \mu_i\big),$$

where σ_i^2 and ψ_i are the variance and the third central moment of the phenotypic distribution, respectively. These two quantities are also dynamical variables, and their dynamics are governed by higher moments of the phenotypic distribution. But this dynamical system is not closed, and these higher moments are also dynamical variables that depend on additional moments. Various approximations, however, have been used to capture its behavior. Typically, many results are based on the Gaussian approximation, which focuses on the dynamics of the mean and the variance and discards all higher cumulants of the distribution (Bürger 2000; Rice 2004). Yet several authors have pointed out that neglecting the skewness of the distribution can underestimate the amount of differentiation and local adaptation Yeaman and Guillaume 2009; Débarre *et al.* 2013, 2015. Indeed, in the case of symmetrical habitats, that is when $m_1 = m_2 = m, \kappa_1 = \kappa_2 = \kappa, s_1 = s_2 = s, r_{\max,1} = r_{\max,2} = r_{\max}$, one can readily obtain the size and the mean trait of the population at equilibrium (the equilibrium is indicated by a superscript *). Using the fact

Table 1 First three moments of the phenotypic distribution at mutation–selection equilibrium in a single population

	Exact value	First approximation	Second approximation
Mean: $\mu_{\varepsilon,0}^*$	−0.29	−0.29	−0.35
Variance: $\sigma_{\varepsilon,0}^{*2}$	0.13	0.14	0.09
Third central moment: $\psi_{\varepsilon,0}^*$	0.02	0.02	0.01

We compare the values from the exact numerical resolution of Equation 5 and our two approximations using the growth rate given in Equation 12 (see also **Figure 2**). Parameter values: $r_{max} = 3$, $s_0 = 1$; $\theta = -0.5$, $\kappa = 1$, $a = 0.2$, $b = 1$, $U = 1$, and $\varepsilon = 0.1$

that $N_1^* = N_2^* = N^*$, $\mu_1^* = -\mu_2^*$, $\sigma_1^* = \sigma_2^* = \sigma^*$ and $\psi_1^* = -\psi_2^* = \psi^*$, we obtain:

$$N^* = \frac{1}{\kappa}\left(r_{max} - s\left(\frac{(2m\theta - s\psi^*)^2}{4(m + g\sigma^{*\,2})^2} + \sigma^{*\,2}\right)\right),$$

$$\mu_1^* = \frac{-s(\psi^* + 2\theta\sigma^{*\,2})}{2(m + s\sigma^{*\,2})}.$$

The differentiation between the two habitats is thus (Figure 1):

$$\mu_2^* - \mu_1^* = \frac{s(\psi^* + 2\theta\sigma^{*\,2})}{m + s\sigma^{*\,2}}. \tag{13}$$

There is, however, no analytic prediction of the magnitude of the different moments of the phenotypic distribution, except in the limiting case when the mutation rate is extremely low (Débarre *et al.* 2013).

Next, we follow the two-step approach we used to obtain the stationary phenotypic distribution in a single population. First, we analyze the evolutionary equilibria of the system when mutations are rare using the Adaptive Dynamics framework. We identify monomorphic or dimorphic globally ESSs. Second, we use these ESSs to derive approximations of the stationary solution of Equation 3 when mutation is more frequent and maintains a standing variance at equilibrium.

Adaptive dynamics and evolutionary stable strategies

We consider a resident population at a demographic equilibrium set by the phenotypic densities of the resident in both habitats (see the supplementary information, Section A.2.1). We want to determine the fate of a mutant with phenotype z_m introduced into this resident population. The ability of the mutant to invade is determined by its fitness, given by:

$$w_i(z_m; N_i) = r_i(z_m) - \kappa_i N_i, \qquad \text{for } i = 1, 2. \tag{14}$$

To take into account migration between habitats, we introduce an effective fitness, which corresponds to the growth rate of a trait in the whole environment (see Caswell 1989; Metz *et al.* 1992; Meszéna *et al.* 1997). The effective fitness $W(z_m; N_1, N_2)$, which corresponds to the *effective* growth rate

associated with trait z_m in the resident population (n_1, n_2), is the largest eigenvalue of the following matrix:

$$\mathcal{A}(z_m; N_1, N_2) = \begin{pmatrix} w_1(z_m; N_1) - m_1 & m_2 \\ m_1 & w_2(z_m; N_2) - m_2 \end{pmatrix}. \tag{15}$$

After some time, the dynamical system will reach a globally stable demographic equilibrium. Because there are two habitats, we expect that, at most, two distinct traits can coexist. With an analysis of the effective fitness W, we characterize such equilibrium corresponding to the evolutionary stable strategy (see the supplementary information, Section A.2.1.1). This equilibrium is indeed either monomorphic (with phenotype z^{M*} and total population size N_i^{M*}) or dimorphic (with phenotypes z_I^{D*} and z_{II}^{D*} and total population size N_i^{D*}, where the subscripts I and II indicate that the phenotype is best adapted to habitat 1 and 2, respectively).

Equilibrium distribution with mutation

In the following, we allow the mutation rate to increase and we study the impact of mutations on the ultimate evolutionary equilibrium of the phenotypic densities, *i.e.*, the stationary solution of Equation 3. We present below the general principle of the approach before examining specific case studies.

As above, we introduce the parameter $\varepsilon = \sqrt{V_m}$ and we approximate the phenotypic density $n_{\varepsilon,i}^*(z)$, the equilibrium of Equation 3 with $V_m = \varepsilon^2$, in terms of ε. Our objective is to provide an approximation of the phenotypic density in each habitat when the effect of mutation (measured by ε) is small, while the mutation rate can be large.

We use analogous transformation to (7):

$$n_{\varepsilon,i}^*(z) = \frac{1}{\sqrt{2\pi\varepsilon}}\exp\left(\frac{u_{\varepsilon,i}(z)}{\varepsilon}\right). \tag{16}$$

Our objective is then to estimate $u_{\varepsilon,i}(z)$. We proceed as in the one-population scenario, and we postulate an expansion for $u_{\varepsilon,i}$ in terms of ε:

$$u_{\varepsilon,i}(z) = u_i(z) + \varepsilon v_i(z) + O(\varepsilon^2), \tag{17}$$

and we try to compute the coefficients $u_i(z)$ and $v_i(z)$. First, we can show that, when there is migration in both directions (*i.e.*, $m_i > 0$ for $i = 1, 2$), the zero-order terms are the same in both habitats: $u_1(z) = u_2(z) = u(z)$ (see the supplementary information, Section A.2.1.2). We can indeed compute explicitly $u(z)$, which is given by (A.23) in the monomorphic case and by (A.24) in the dimorphic case. As we observe in the equations (A.23) and (A.24), $u(z)$ attains its maximum (which is equal to 0) at the ESS points identified in the previous subsection. This means that the peaks of population distribution are around the ESS points (z^{M*} in the case of the monomorphic ESS and (z_I^{D*}, z_{II}^{D*}) for the dimorphic ESS). Note that the fact that $u_1(z) = u_2(z) = u(z)$ means that the peaks of the population distribution are placed approximately at the same points (ESS points) in both habitats.

However, the size of the peaks may be different since $v_1(z)$ is not necessarily equal to $v_2(z)$.

We are also able to compute the first-order term $v_i(z)$ (see the supplementary information, Section A.2.1.2). This allows us to obtain a *first approximation* of the phenotypic density $n^*_{\varepsilon,i}(z)$. This approximation of the stationary distribution is very accurate (see, for instance, Figure 4).

As in the one population scenario, we derive more explicit formula for the moments of order $k \geq 1$ of the stationary phenotypic distribution. This *second approximation*, instead of using the values of $u(z)$ and $v_i(z)$ in the whole domain, is based on the computation of the Taylor expansions of $u(z)$ and $v_i(z)$ around the ESS points (see the supplementary information, Section A.2.1.3).

Case studies

Symmetric fitness landscapes: We focus first on a symmetric scenario, where, apart from the position of the optimum, the two habitats are identical: $m_1 = m_2 = m, \kappa_1 = \kappa_2 = \kappa, s_1 = s_2 = s, r_{\max,1} = r_{\max,2} = r_{\max}$. In this special case, it is possible to fully characterize the evolutionary equilibrium.

When migration rate is higher than the critical migration threshold:

$$m > m_c = 2s\theta^2 \qquad (18)$$

migration prevents the differentiation of the trait between the two habitats (see the supplementary information, Subsection A.2.1.1). The only evolutionary equilibrium, when the mutation rate is vanishingly small, is monomorphic, and satisfies $z^{M*} = 0$ and $n_1^{M*}(z) = n_2^{M*}(z) = N^{M*}\delta(z)$, where $\delta(.)$ is the dirac delta function and $N^{M*} = \frac{1}{\kappa}(r_{\max} - s\theta^2)$.

Monomorphic case: Let us suppose that $m_c = 2s\theta^2 \leq m$. Then, $z^{M*} = 0$ is the only ESS and $N^{M*} = \frac{1}{\kappa}(r_{\max} - s\theta^2)$. Then, we can provide our *first approximation* of the phenotypic density $n_{\varepsilon,i}(z)$ following the method introduced above (Figure 3). Moreover, defining $\phi = \sqrt{1 - 2s\theta^2/m}$, we can use the *second approximation* to obtain an analytic formula for the moments of the stationary state:

$$
\begin{cases}
N^{M*}_{\varepsilon,1} = N^{M*}_{\varepsilon,2} = \int n^{M*}_{\varepsilon,i}(z)dz = \dfrac{1}{\kappa}(r_{\max} - s\theta^2) - \varepsilon\dfrac{\sqrt{Us}\,\phi}{\kappa} + O(\varepsilon^2), \\[2ex]
\mu^{M*}_{\varepsilon,1} = \dfrac{1}{N^{M*}_{\varepsilon,1}} \int z n^{M*}_{\varepsilon,1}(z)dz = -\varepsilon\dfrac{\sqrt{Us}\,\theta}{m\phi} + O(\varepsilon^2), \\[2ex]
\mu^{M*}_{\varepsilon,2} = \dfrac{1}{N^{M*}_{\varepsilon,2}} \int z n^{M*}_{\varepsilon,2}(z)dz = \varepsilon\dfrac{\sqrt{Us}\,\theta}{m\phi} + O(\varepsilon^2), \\[2ex]
\sigma^{M*\,2}_{\varepsilon,1} = \sigma^{M*\,2}_{\varepsilon,2} = \dfrac{1}{N^{M*}_{\varepsilon,i}} \int \left(z - \mu^{M*}_{\varepsilon,i}\right)^2 n^{M*}_{\varepsilon,i}(z)dz = \dfrac{\varepsilon\sqrt{U}}{\sqrt{s}\phi} + O(\varepsilon^2), \\[2ex]
\psi^{M*}_{\varepsilon,i} = \dfrac{1}{N^{M*}_{\varepsilon,i}} \int \left(z - \mu^{M*}_{\varepsilon,i}\right)^3 n^{M*}_{\varepsilon,i}(z)dz = O(\varepsilon^3).
\end{cases}
$$
$$(19)$$

These results are consistent with Equation 13. Note that the equilibrium variance in each habitat, $\sigma^{M*2}_{\varepsilon,i} \approx \frac{\varepsilon\sqrt{U}}{\sqrt{s}\phi}$, is larger
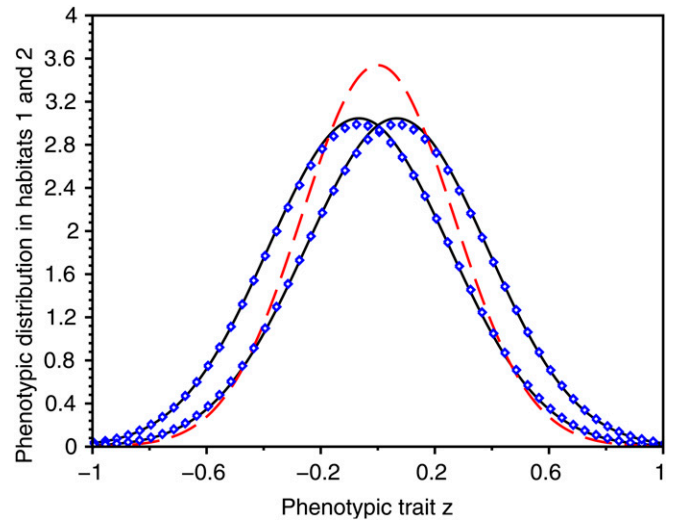

Figure 3 Selection–mutation–migration equilibrium of the phenotypic densities $n_{\varepsilon,i}(z)$ in the two habitats in a symmetric scenario. We plot the exact phenotypic densities at equilibrium obtained from numerical computations of the equilibrium of Equation 3 (blue dots) together with our *first approximation* (full black line) in a case where the distribution is unimodal in each habitat. We also plot the approximation given in Débarre *et al.* (2013) (red dashed line). Note that our approximation captures the emergence of some differentiation, even though we are above the critical migration rate leading to the evolution of a dimorphic population. In the presence of large mutation rates, the population distribution is indeed shifted to the left (respectively right) in the first (respectively second) habitat, while Débarre *et al.* (2013) provided the same approximation for both habitats. Our calculation yields also better approximations for the variance of the distribution in each habitat (Débarre *et al.* 2013 underestimates this variance). In this and the following figures, to compute the equilibrium numerically, we have solved the dynamic problem numerically (Equation 3) and kept the solution obtained for a long time after equilibrium has been reached. Parameter values: $m = 1.5$, $r_{\max} = 3$, $s = 2$; $\theta = 0.5$, $\kappa = 1$, $U = 1$, $\varepsilon = 0.1$.

than the equilibrium variance maintained in the absence of heterogeneity between the habitats (*cf*. Equation 11). This increase in the equilibrium variance comes from ϕ, which depends on dispersion and the heterogeneity between the two habitats. The variance of the distribution increases as ϕ decreases. When $\phi = 0$, the approximation for the variance becomes infinitely large. Indeed, this corresponds to the threshold value of migration, below which the above approximation collapses because the distribution becomes bimodal. In this case, we have to switch to analysis of the dimorphic case. Note that the differentiation between habitats also depends on ϕ. Some differentiation emerges even when the migration rate is above the critical migration rate, m_c (Figures 3 and 4). In Figure 4 we provide a comparison of the results from the *first* and the *second approximations*. Our *second approximation* yields convincing results when the parameters are such that we are far from the transition zone from monomorphic to dimorphic distribution. This approximation is indeed based on an integral approximation, which is relevant only when the population distribution is relatively sharp around the ESS points. This is not the case in the transition zone unless the effect of the mutations, *i.e.*, ε, is very small.
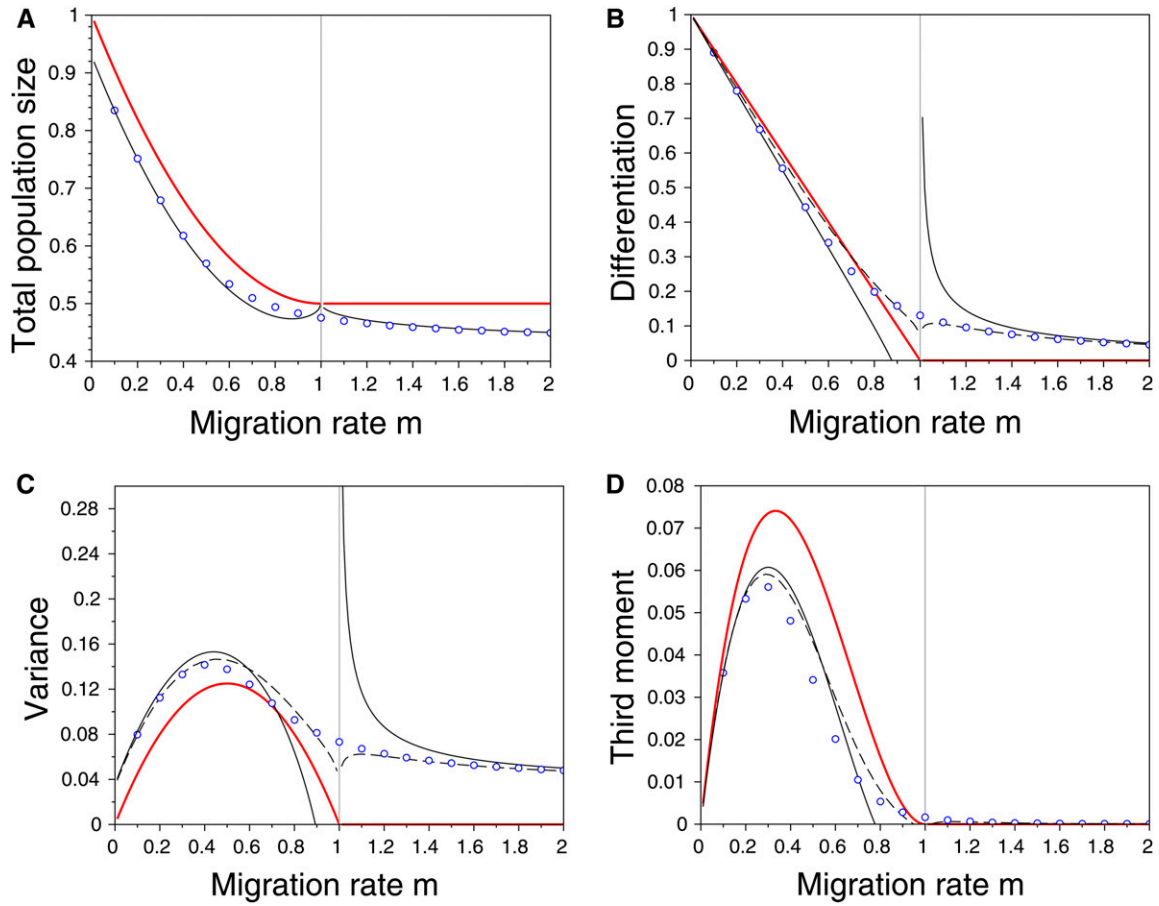
Figure 4 Effects of migration in a symmetric scenario on (A) the total population size ($N^*_{\varepsilon,1}$) in habitat 1, (B) the differentiation between habitats ($\mu^*_{\varepsilon,2} - \mu^*_{\varepsilon,1}$), (C) the variance ($\sigma^{*2}_{\varepsilon,1}$), and (D) the third central moment of the phenotypic distribution ($\psi^*_{\varepsilon,1}$) in habitat 1 (see Equation 19 and Section B.3 for the definition of these quantities and the analytic formula obtained from our *second approximation*). The dots refer to the numerical resolutions of the problem with $\varepsilon = 0.05$, the red line indicates the case where $\varepsilon = 0$, while the lines in black refer to our two approximations when $\varepsilon = 0.05$ (the dashed line for the *first approximation* and the full line for the *second approximation*). The vertical gray line indicates the critical migration rate below which dimorphism can evolve in the Adaptive Dynamics scenario. Note that both approximations predict the same total population size. Other parameter values: $r_{max} = 1$, $s = 2$, $\theta = 0.5$, $\kappa = 1$, and $U = 1$.

Dimorphic case: When $m < m_c$, the only globally stable evolutionary equilibrium is dimorphic, which yields the following ESS: $\{z^{D*}_{\mathrm{I}}, z^{D*}_{\mathrm{II}}\}$ with $z^{D*}_{\mathrm{I}} = -z^{D*}_{\mathrm{II}} = -z^{D*}$ and $z^{D*} = \frac{\sqrt{4s^2\theta^4 - m^2}}{2s\theta}$. When $\varepsilon = 0$, this yields the following phenotypic densities at equilibrium: $n^{D*}_i(z) = \nu_{\mathrm{I},i}\delta(z - z^{D*}_{\mathrm{I}}) + \nu_{\mathrm{II},i}\delta(z - z^{D*}_{\mathrm{II}})$ (analytic expressions for $\nu_{\mathrm{I},j}$ and $\nu_{\mathrm{II},j}$ are given in the supplementary information, Section B.1). When $\varepsilon > 0$, we can use our *first* and *second approximations* to obtain convincing approximations of the phenotypic distribution and its moments (see Figure 4). Our *first approximation* improves the Adaptive Dynamics predictions in a broad range of the parameter space, and, as pointed out above, our *second approximation* is pertinent when the parameters are such that we are far from the transition zone from dimorphic to monomorphic distribution. The analytic expressions for the local moments of the stationary distribution in each habitat, obtained from our *second approximation*, are given in the supplementary information, Section B.3.

Nonsymmetric scenarios: A general nonsymmetric scenario: In a nonsymmetric scenario, there is also a unique globally stable evolutionary strategy that is either monomorphic or dimorphic. There is still a threshold value of migration, above which the maintenance of a dimorphic polymorphism is impossible: $\Delta = \frac{m_1 m_2}{4s_1 s_2 \theta^4} \geq 1$. Note that this condition generalizes the condition in the symmetric case (i.e., when $m_1 = m_2$ and $s_1 = s_2$). However, for the ESS to be dimorphic, the condition $\Delta < 1$ is not enough and two other conditions should also be satisfied. These conditions (i.e., $\eta_1 < \beta_2 r_{max,2} - \alpha_1 r_{max,1}$ and $\eta_2 < \beta_1 r_{max,1} - \alpha_2 r_{max,2}$ with the constants α_i, β_i and η_i depending on the parameters $m_1, m_2, s_1, s_2, \kappa_1, \kappa_2$ and θ, see the supplementary information, Section B.2) guarantee that the qualities of the habitats are not very different. Indeed, if one habitat has a higher quality it is likely to overwhelm the dynamics of adaptation in the other habitat. This will yield a monomorphic equilibrium biased toward the high-quality habitat. Figure 5 illustrates that a polymorphism is maintained only in a range of parameter values where the two habitats are
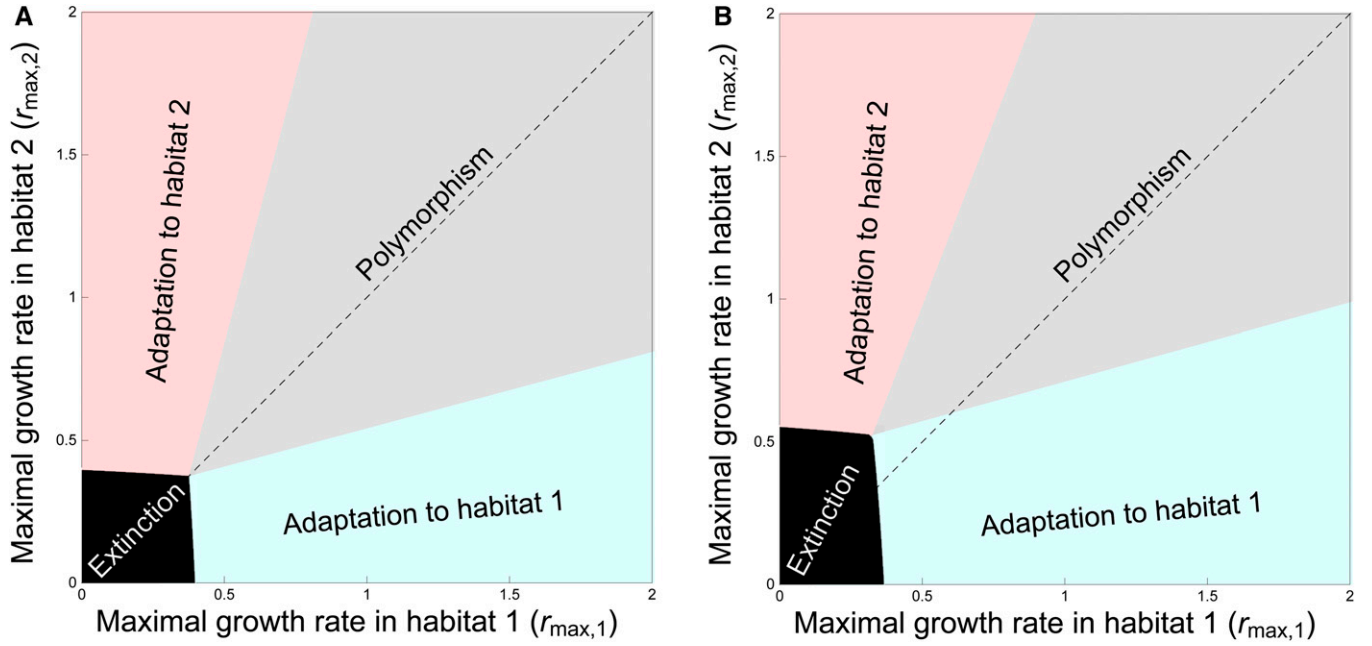
Figure 5 Maintenance of polymorphism and nonsymmetric adaptation as a function of the maximal growth rates $r_{max,1}$ and $r_{max,2}$ in the two habitats. In (A) we examine a symmetric situation where all the parameters are identical in the two habitats: $m_1 = m_2 = 0.5$, $s_1 = s_2 = 2$, and $\kappa_1 = \kappa_2 = 1$. In (B) we show a nonsymmetric case with the same parameters as in (A) except $m_1 = 0.5$ and $m_2 = 0.7$. The black area indicates the parameter space, where the population is driven to extinction because the maximal growth rates are too low. In the gray area, some polymorphism can be maintained in the two-habitat population as long as the difference in the maximal growth rates are not too high. When this difference reaches a threshold, polymorphism cannot be maintained and the single type that is maintained is more adapted to the good-quality habitat (the habitat with the highest maximal growth rate).

relatively similar. Interestingly, in spite of the asymmetry of the two habitats, the locations of the two peaks of the phenotypic distribution are always symmetric, and, consequently, $z_1^{D*} = -z_2^{D*} = -z^{D*}$, where: $z^{D*} = \sqrt{\theta^2(1-\Delta)}$. The symmetric locations of the peaks is indeed a consequence of the choice of the quadratic stabilizing selection (Equation 1). See the supplementary information, Section B.1 for the expressions of the densities in each habitat, and Section A.2.1.1 for the conditions leading to this stable equilibrium.

A source–sink scenario: An extreme case of asymmetry occurs when one population (the source) does not receive any migrant from the second population (the sink). For instance, when $m_1 > 0$ and $m_2 = 0$, there is no immigration in habitat 1. Note that this is a degenerate case. In contrast with the above analysis, where both m_1 and m_2 are positive, we have to provide an analysis of ESS for each habitat separately. Moreover, computation of the equilibrium in presence of mutations is slightly different because of this degeneracy (see the supplementary information Section A.2.2).

The evolutionary outcome in the first habitat is obvious because it depends only on selection acting in habitat 1: the ESS is $-\theta$ and

$$N_1^* = \frac{r_{max,1} - m_1}{\kappa_1}. \tag{20}$$

Moreover, the population's phenotypic density, $n_{\varepsilon,1}^*$, can be computed explicitly: $n_{\varepsilon,1}^* = N_{\varepsilon,1}^* f_\varepsilon$, where $N_{\varepsilon,1}^* = \frac{r_{max,1} - m_1 - \varepsilon\sqrt{Us_1}}{\kappa_1}$ and

f_ε is the probability density of a normal distribution $\mathcal{N}\left(-\theta, \frac{\varepsilon\sqrt{U}}{\sqrt{s_1}}\right)$.

In habitat 2, the evolutionary outcome results from the balance between migration from habitat 1 and local selection. Interestingly, migration has a nonmonotonic effect on adaptation in the sink (See Figure 6). Indeed, Figure 6A shows that the population size in the sink is maximized for intermediate values of migration. More migration from the source has a beneficial effect on the demography of the sink, but it prevents local adaptation. Yet, when migration from the source becomes very large it limits the size of the population in the source (see Equation 20). This limits the influence of the source on the sink, and can even promote adaptation to the sink. In fact, it is worth noting that differentiation between the two habitats can actually increase with migration (Figure 6B). The level of migration from the source that prevents local adaptation in the sink is given by the condition:

$$\frac{4s_2\theta^2 r_{max,2}}{\kappa_2} \leq \frac{m_1(r_{max,1} - m_1)}{\kappa_1}. \tag{21}$$

Indeed, when condition Equation 21 is verified, the migration from the source overwhelms local selection, and the evolutionary stable strategy in the sink is $z^* = -\theta$. In contrast, when condition Equation 21 does not hold, the effective growth rate of the optimal trait θ in the sink habitat is high enough to compete with the trait $-\theta$ coming from the source, allowing coexistence between the two strategies. Note again
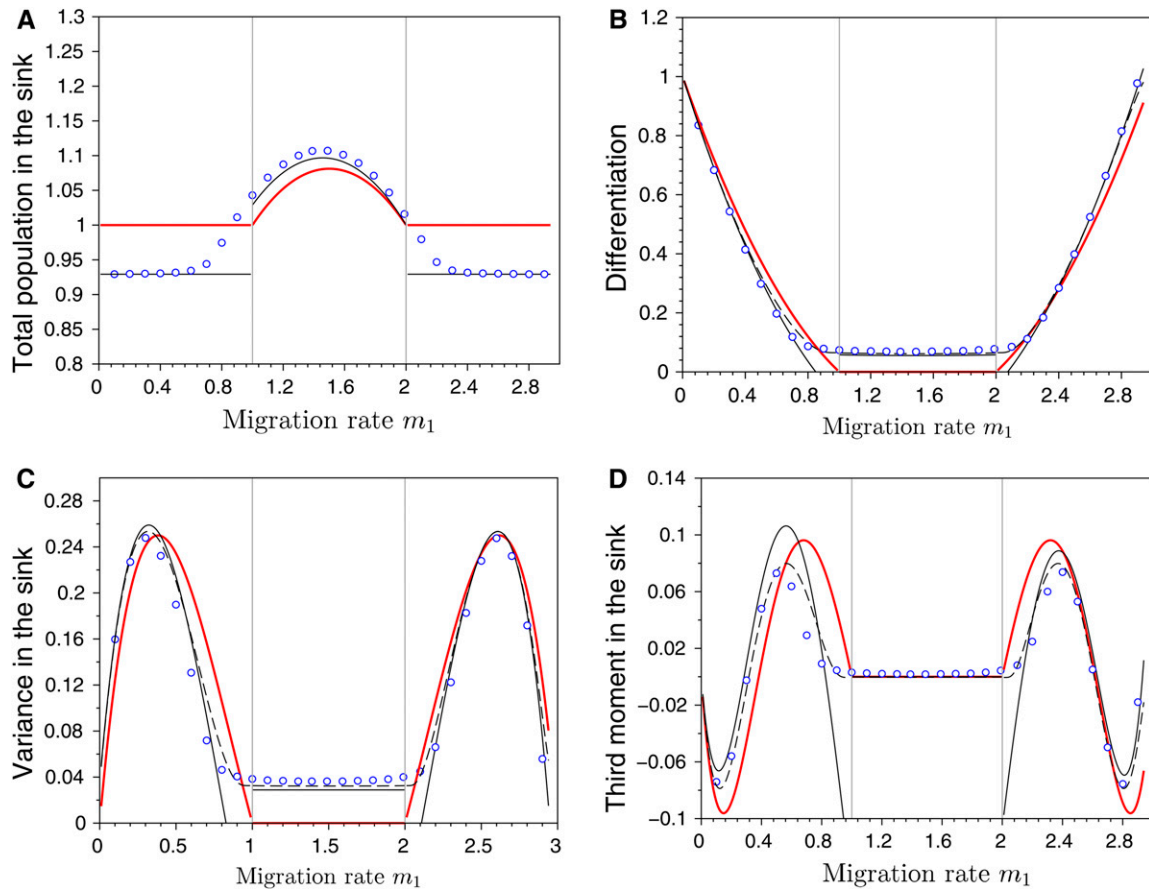
Figure 6 Effects of migration in a source–sink scenario on (A) the total population size in the sink habitat, (B) the differentiation between habitats, (C) the variance, and (D) the third central moment of the phenotypic distribution in sink. The dots refer to exact numerical computations when $\varepsilon = 0.05$, the red line indicates the case where $\varepsilon = 0$ while the lines in black refer to our two approximations when $\varepsilon = 0.05$ (dashed line for the *first approximation* and the full line for the *second approximation*). The vertical gray lines, at $m_1 = 1$ and $m_1 = 2$, indicate the critical migration rates where transition occurs between monomorphism and dimorphism in the Adaptive Dynamics framework (see condition Equation 21). Note that both approximations predict the same total population size. Other parameter values: $r_{\max,1} = 3$, $r_{\max,2} = 1$, $s_1 = 3$, $s_2 = 2$, $\kappa_1 = \kappa_2 = 1$, $\theta = 0.5$, and $U = 1$.

that our two approximations (see supplementary information sections A.2.2.2 for the derivation of the *first approximation* and B.4 for the analytic formula for the moments of the phenotypic distribution derived from our *second approximation*) provide very good predictions for the moments of the phenotypic distribution in the sink (Figure 6).

Discussion

The balance between selection, migration, and mutation drives the dynamics of local adaptation in heterogeneous environments. Here, we present a new theoretical approach to obtain accurate approximations for the equilibrium phenotypic densities in a two-habitat environment. This analysis goes beyond the Adaptive Dynamics framework because it allows us to account for the effect of large mutation rates. This analysis does not rely on the Gaussian approximation that underlies many Quantitative Genetics models. Our analysis yields analytic approximations that help provide a good understanding of the balance between the different evolutionary forces in both *symmetric* and *nonsymmetric* scenarios.

In the *symmetric* scenario, we recover the classical results from Quantitative Genetics in a single population (Lande 1975; Bürger 2000; Rice 2004) but expand this to spatially heterogeneous scenarios. In particular, we capture the emergence of differentiation between habitats when the migration rate decreases. When migration is strong relative to selection, the stationary phenotypic density is unimodal in each habitat but heterogeneous selection increases phenotypic variance and differentiation (see Equation 19 and Figure 4). When migration is close to the critical migration rate m_c (see condition Equation 18), we observe a shift between the phenotypic distributions of the two habitats. This pattern was not detected in previous studies, but our method captures this shift and improves the approximation of the variance of the phenotypic distributions [see Débarre *et al.* (2013) and Figure 3]. When the migration rate is much smaller than m_c, and selection is sufficiently strong between habitats, the equilibrium distribution in each habitat can be well approximated as the sum of two distributions. But, unlike previous approximations (Yeaman and Guillaume 2009; Débarre *et al.* 2013) these two distributions are non-Gaussian. We derive

approximations for the moments of these distributions. In other words, this work generalizes previous attempts to derive the distribution of a phenotypic trait at the mutation–selection–migration equilibrium. Our results confirm the importance of the skewness in the phenotypic distribution, and improve predictions of measures of local adaptation in a heterogeneous environment.

In the *nonsymmetric* scenario, we show that the condition for the maintenance of two specialized strategies is more restrictive (Figure 5). Indeed, asymmetries promote a single strategy that is more locally adapted to the habitat with larger population size and/or lower immigration rate. The impact of biased migration rates from a source population into the adaptation of peripheral populations has been discussed before (Holt and Gaines 1992; García-Ramos and Kirkpatrick 1997; Gomulkiewicz *et al.* 1999; Holt *et al.* 2003; Akerman and Bürger 2014). Our approach, however, yields a quantitative description of the shape of the phenotypic distributions in both the source and the sink habitats. These accurate predictions are key to understanding the effect of different evolutionary forces on the level of adaptation in the two habitats. For instance, the analysis of an extreme case with source–sink dynamics reveals the complex interplay between migration, demography, and local selection. The maintenance of a polymorphic equilibrium is possible when migration from the source is either very weak or very strong. This result challenges the classical prediction where migration is always a homogenizing force reducing the differentiation among populations (Figure 6).

Our work illustrates the potential of a new mathematical tool in the field of evolutionary biology. In this work, we use an approach based on Hamilton-Jacobi equations [see (A.22)], which has been developed, mostly by the mathematical community, during the last decade to describe the asymptotic solutions of selection–mutation models, as the effect of mutation vanishes. We refer to Diekmann *et al.* (2005), Perthame and Barles (2008), and Mirrahimi (2011) for the establishment of the basis of this approach. Note, however, that previous studies were focused mainly on the limit case where the effects of mutations are vanishingly small. In particular, they do not provide approximations of phenotypic density and its moments when the effect of mutations, ε, is nonzero. In the present work, we go further than the previous studies and characterize the phenotypic distributions when the influx of mutations can alter significantly the shape of the stationary distribution. Understanding the build up of this distribution is particularly important when studying the effect of mutation on adaptation. Although mutation is the ultimate source of adaptive variation, the accumulation of deleterious mutations generates a load on the average fitness of populations. This is particularly relevant in organisms like RNA viruses that are characterized by very large mutation rates (Drake and Holland 1999; Sanjuán *et al.* 2010). In fact, the mutation loads of RNA virus is so high that it may even lead some populations to extinction (Bull *et al.* 2007; Martin and Gandon 2010). Our model can be used to accurately
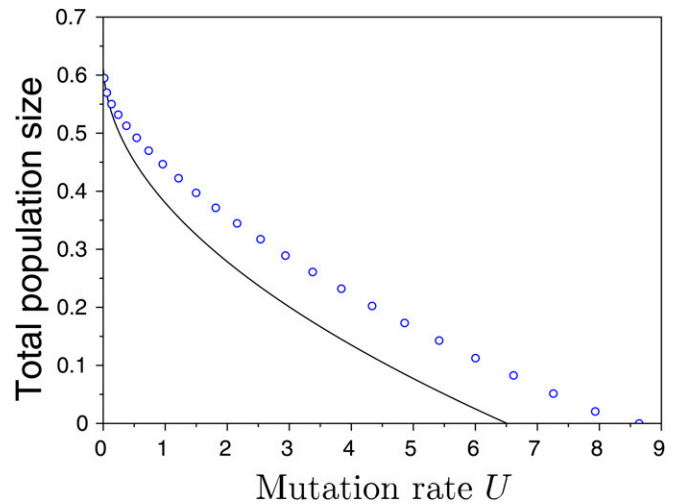

Figure 7 Effect of increasing the mutation rate U on the total population size in the symmetric scenario used in Figure 3 with $m = 0.5$. The full line indicates the approximation, and the dots are the results of exact numerical computations. This figure illustrates that our approximation given by the first line of Equation 19 captures reasonably well the effect of large mutation rates on the mutation load in a two-habitat scenario where there is differentiation and some local adaptation.

capture the effect of increasing mutation rates on the mutation load of a population living in a heterogeneous environment (Figure 7). This heterogeneity may be particularly relevant in chronic infections by pathogenic viruses that can adapt to different organs (Kemal *et al.* 2003; Ducoulombier *et al.* 2004; Sanjuán *et al.* 2004; Jridi *et al.* 2006). A better understanding of the phenotypic distribution at equilibrium in heterogeneous environments may thus provide more accurate prediction on the critical mutation rates that can ultimately lead within-host dynamics to pathogen extinction.

Our analysis of the equilibrium between selection, migration, and mutation could be extended in several new directions. More than two habitats could be considered, or different growth rates and/or mutation kernels could be used [see Mirrahimi (2013) and the supplementary information, Section (A.3)]. The approach could also be used to analyze situations away from the equilibrium. For instance, it would be possible to track the dynamics of the distribution as the population adapts to a new environment, or to a time-varying environment (Lande and Shannon 1996). Hamilton-Jacobi equations have indeed also been used to study time-varying (but space homogeneous) environments (see, for instance, Mirrahimi *et al.* 2015; Figueroa Iglesias and Mirrahimi 2018). Finally, it is interesting to note that the generalization of the present ecological scenario to model the adaptation of sexual species in heterogeneous environments remains to be carried out. Our method could be extended to allow for sexual reproduction within the framework of the infinitesimal model (see Fisher 1919; Calvez *et al.* 2019). But this analysis falls beyond the scope of the present paper.

Acknowledgments

Literature Cited

Akerman, A., and R. Bürger, 2014 The consequences of gene flow for local adaptation and differentiation: a two-locus two-deme model. J. Math. Biol. 68: 1135–1198. https://doi.org/10.1007/s00285-013-0660-z

Barles, G., S. Mirrahimi, and B. Perthame, 2009 Concentration in Lotka-Volterra parabolic or integral equations: a general convergence result. Methods Appl. Anal. 16: 321–340.

Bull, J. J., R. Sanjuan, and C. O. Wilke, 2007 Theory of lethal mutagenesis for viruses. J. Virol. 81: 2930–2939. https://doi.org/10.1128/JVI.01624-06

Bürger, R., 2000 *The Mathematical theory of selection, recombination and mutation*. Wiley, New-York.

Calvez, V., J. Garnier, and F. Patout, 2019 A quantitative genetics model with sexual mode of reproduction in the regime of small variance. arXiv: 1811.01779v3.

Caswell, H., 1989 *Matrix Population Models*, Sinauer Associates, Sunderland, MA.

Champagnat, N., R. Ferrière, and S. Méléard, 2008 Individual-based probabilistic models of adaptive evolution and various scaling approximations. Progress in Probability 59: 75–113. https://doi.org/10.1007/978-3-7643-8458-6_6

Christiansen, F. B., 1975 Hard and soft selection in a subdivided population. Am. Nat. 109: 11–16. https://doi.org/10.1086/282970

Day, T., 2000 Competition and the effect of spatial resource heterogeneity on evolutionary diversification. Am. Nat. 155: 790–803. https://doi.org/10.1086/303356

Débarre, F., and S. Gandon, 2010 Evolution of specialization in a spatially continuous environment. J. Evol. Biol. 23: 1090–1099. https://doi.org/10.1111/j.1420-9101.2010.01966.x

Débarre, F., O. Ronce, and S. Gandon, 2013 Quantifying the effects of migration and mutation on adaptation and demography in spatially heterogeneous environments. J. Evol. Biol. 26: 1185–1202. https://doi.org/10.1111/jeb.12132

Débarre, F., S. Yeaman, and F. Guillaume, 2015 Evolution of quantitative traits under a migration-selection balance: when does skew matter? Am. Nat. 186: S37–S47. https://doi.org/10.1086/681717

Diekmann, O., P.-E. Jabin, S. Mischler, and B. Perthame, 2005 The dynamics of adaptation: an illuminating example and a Hamilton-Jacobi approach. Th. Pop. Biol. 67: 257–271. https://doi.org/10.1016/j.tpb.2004.12.003

Doebeli, M., and U. Dieckmann, 2003 Speciation along environmental gradients. Nature 421: 259–264. https://doi.org/10.1038/nature01274

Drake, J. W., and J. Holland, 1999 Mutation rates among RNA viruses. Proc. Natl. Acad. Sci. USA 96: 13910–13913. https://doi.org/10.1073/pnas.96.24.13910

Ducoulombier, D., A.-M. Roque-Afonso, G. Di Liberto, F. Penin, R. Kara *et al.*, 2004 Frequent compartmentalization of hepatitis c virus variants in circulating B cells and monocytes. Hepatology 39: 817–825. https://doi.org/10.1002/hep.20087

Figueroa Iglesias, S., and S. Mirrahimi, 2018 Long time evolutionary dynamics of phenotypically structured populations in fluctuating environments. SIAM J. Math. Anal. 50: 5537–5568. https://doi.org/10.1137/18M1175185

Fisher, R. A., 1919 Xv.-the correlation between relatives on the supposition of Mendelian inheritance. Earth and Environmental Science Transactions of the Royal Society of Edinburgh 52: 399–433. https://doi.org/10.1017/S0080456800012163

Gandon, S., and S. Mirrahimi, 2017 A Hamilton-Jacobi method to describe the evolutionary equilibria in heterogeneous environments and with non-vanishing effects of mutations. C. R. Math. 355: 155–160. https://doi.org/10.1016/j.crma.2016.12.001

García-Ramos, G., and M. Kirkpatrick, 1997 Genetic models of adaptation and gene flow in peripheral populations. Evolution 51: 21–28. https://doi.org/10.1111/j.1558-5646.1997.tb02384.x

Geritz, S. A. H., E. Kisdi, G. Mészena, and J. A. J. Metz, 1998 Evolutionarily singular strategies and the adaptive growth and branching of the evolutionary tree. Evol. Ecol. 12: 35–57. https://doi.org/10.1023/A:1006554906681

Gomulkiewicz, R., R. D. Holt, and M. Barfield, 1999 The effects of density dependence and immigration on local adaptation and niche evolution in a black-hole sink environment. Th. Pop. Biol. 55: 283–296. https://doi.org/10.1006/tpbi.1998.1405

Holt, R. D., and M. S. Gaines, 1992 Analysis of adaptation in heterogeneous landscapes: implications for the evolution of fundamental niches. Evol. Ecol. 6: 433–447. https://doi.org/10.1007/BF02270702

Holt, R. D., R. Gomulkiewicz, and M. Barfield, 2003 The phenomenology of niche evolution via quantitative traits in a 'black-hole' sink. Proc. R. Soc. Lond. B Biol. Sci. 270: 215–224. https://doi.org/10.1098/rspb.2002.2219

Jridi, C., J.-F. Martin, V. Marie-Jeanne, G. Labonne, and S. Blanc, 2006 Distinct viral populations differentiate and evolve independently in a single perennial host plant. J. Virol. 80: 2349–2357. https://doi.org/10.1128/JVI.80.5.2349-2357.2006

Kemal, K. S., B. Foley, H. Burger, K. Anastos, H. Minkoff *et al.*, 2003 Hiv-1 in genital tract and plasma of women: compartmentalization of viral sequences, coreceptor usage, and glycosylation. Proc. Nat. Aca. Sci. USA. 100: 12972–12977. https://doi.org/10.1073/pnas.2134064100

Kimura, M., 1965 A stochastic model concerning the maintenance of genetic variability in quantitative characters. Proc. Natl. Acad. Sci. USA 54: 731–736. https://doi.org/10.1073/pnas.54.3.731

Lande, R., 1975 The maintenance of genetic variability by mutation in a polygenic character with linked loci. Genet. Res. 26: 221–235. https://doi.org/10.1017/S0016672300016037

Lande, R., and S. Shannon, 1996 The role of genetic variation in adaptation and population persistence in a changing environment. Evolution 50: 434–437. https://doi.org/10.1111/j.1558-5646.1996.tb04504.x

Leimar, O., M. Doebeli, and U. Dieckmann, 2008 Evolution of phenotypic clusters through competition and local adaptation along an environmental gradient. Evolution 62: 807–822. https://doi.org/10.1111/j.1558-5646.2008.00334.x

Lenormand, T., 2002 Gene flow and the limits to natural selection. Trends Ecol. Evol. 17: 183–189. https://doi.org/10.1016/S0169-5347(02)02497-7

Martin, G., and S. Gandon, 2010 Lethal mutagenesis and evolutionary epidemiology. Philos. Trans. R. Soc. Lond. B Biol. Sci. 365: 1953–1963. https://doi.org/10.1098/rstb.2010.0058

Meszéna, G., I. Czibula, and S. Geritz, 1997 Adaptive dynamics in a 2-patch environment: a toy model for allopatric and parapatric speciation. J. Biol. Syst. 5: 265–284. https://doi.org/10.1142/S0218339097000175

Metz, J. A. J., R. M. Nisbet, and S. A. H. Geritz, 1992 How should we define 'fitness' for general ecological scenarios? Trends Ecol. Evol. 7: 198–202. https://doi.org/10.1016/0169-5347(92)90073-K

Mirrahimi, S., 2011   *Concentration phenomena in PDEs from biology.* PhD thesis, University of Pierre et Marie Curie, Paris, France.

Mirrahimi, S., 2013   Migration and adaptation of a population between patches. Discrete Continuous Dyn. Syst. Ser. B 18: 753–768. https://doi.org/10.3934/dcdsb.2013.18.753

Mirrahimi, S., 2017   A Hamilton-Jacobi approach to characterize the evolutionary equilibria in heterogeneous environments. Math. Models Methods Appl. Sci. 27: 2425–2460. https://doi.org/10.1142/S0218202517500488

Mirrahimi, S., B. Perthame and P. E. Souganidis, 2015   Time fluctuations in a population model of adaptive dynamics. Annales de l'I.H.P. Analyse non linéaire 32: 41–58. https://doi.org/10.1016/j.anihpc.2013.10.001

Nagylaki, T., 1978   A diffusion model for geographically structured populations. J. Math. Biol. 6: 375–382. https://doi.org/10.1007/BF02463002

Perthame, B., and G. Barles, 2008   Dirac concentrations in Lotka-Volterra parabolic PDEs. Indiana Univ. Math. J. 57: 3275–3302. https://doi.org/10.1512/iumj.2008.57.3398

Rice, S. H., 2004   *Evolutionary theory: mathematical and conceptual foundations*, Sinauer Associates, Inc., Sunderland, MA

Ronce, O., and M. Kirkpatrick, 2001   When sources become sinks: migration meltdown in heterogeneous habitats. Evolution 55: 1520–1531. https://doi.org/10.1111/j.0014-3820.2001.tb00672.x

Sanjuán, R., F. M. Codoñer, A. Moya, and S. F. Elena, 2004   Natural selection and the organ-specific differentiation of hiv-1 v3 hypervariable region. Evolution 58: 1185–1194. https://doi.org/10.1111/j.0014-3820.2004.tb01699.x

Sanjuán, R., M. Nebot, N. Chirico, L. Mansky, and R. Belshaw, 2010   Viral mutation rates. J. Virol. 84: 9733–9748. https://doi.org/10.1128/JVI.00694-10

Savolainen, O., M. Lascoux, and J. Merilä, 2013   Ecological genomics of local adaptation. Nat. Rev. Genet. 14: 807–820. https://doi.org/10.1038/nrg3522

Slatkin, M., 1978   Spatial patterns in the distributions of polygenic characters. J. Theor. Biol. 70: 213–228. https://doi.org/10.1016/0022-5193(78)90348-X

Szilágyi, A., and G. Meszéna, 2009   Two-patch model of spatial niche segregation. Evol. Ecol. 23: 187–205. https://doi.org/10.1007/s10682-007-9212-6

Whitlock, M. C., 2015   Modern approaches to local adaptation. Am. Nat. 186: S1–S4. https://doi.org/10.1086/682933

Yeaman, S., and F. Guillaume, 2009   Predicting adaptation under migration load: the role of genetic skew. Evolution 63: 2926–2938. https://doi.org/10.1111/j.1558-5646.2009.00773.x

Communicating editor: J. Hermisson